INTERACTION OF RED BLOOD CELLS
WITH A POLARIZED ELECTRODE

EVIDENCE OF LONG-RANGE INTERMOLECULAR FORCES

D. GINGELL *and* J. A. FORNÉS

From the Department of Biology as Applied to Medicine, The Middlesex Hospital Medical School, London, W1 P 6DB, England. Dr. Fornés address is Universidade de São Paulo, Instituto de Fisica e Quimica de São Carlos, Campus de São Carlos, São Carlos (SP), Brazil.

ABSTRACT   We have investigated the electrostatic interaction of glutaraldehyde-fixed human red cells with a polarizable electrode carrying a defined surface charge density which can be varied continuously through a wide range. Cells in a dilute salt solution are unable to adhere to the electrode at high negative charge, but at lower negative charge densities they are reversibly adherent and can be forced off by increasing the negative polarization. Near zero electrode charge they become irreversibly stuck to the electrode and cannot be evicted even at maximum electrode polarization. Calculation of the electrostatic repulsive force using measured charge densities indicates the existence of an attractive force which may be acting over several hundred angstroms.

INTRODUCTION

Our objective is to investigate intermolecular forces between red blood cells and a well defined surface. Bangham and Pethica (1960) and Curtis (1960, 1962) posed the question of whether cell adhesion is subject to the physical forces of electrostatic repulsion and Van der Waals attraction believed to govern the behavior of colloidal particles. Despite several attempts to test this idea, no very clear conclusions have been reached in the intervening decade. This has been due to the extreme complexity of the experimental variables commonly encountered. Even the simplest correlation between adhesiveness and surface electric charge density has proved remarkably elusive (Weiss, 1968a,b; Gingell and Garrod, 1969; Kemp, 1970; Marudas, 1975; see Curtis, 1967, for earlier work) and lack of hard evidence has not encouraged skeptics to moderate their criticisms of the physical force concept.

Advances in the theory of Van der Waals (electrodynamic) forces (Parsegian and Ninham, 1969; Ninham and Parsegian, 1970) based on the method of Lifshitz (1956) have made it possible to calculate long-range attractive forces from spectroscopic data (Gingell and Parsegian, 1972) and to make predictions about the forces of cell adhesion using data for biological materials. These admittedly provisional calculations suggest that appreciable attractive forces exist (Parsegian and Gingell, 1973). Their important

role in the stability of lipid-water systems is becoming apparent from X-ray analysis of lechithin lamellae (Le Neveu et al., 1976) where our theoretical predictions have been supported.

We have attempted to test the hypothesis that attractive electrodynamic and repulsive electrostatic forces underlie the adhesive behavior of biological cells, insofar as it is possible to make precise quantitative physical measurements on such complex bodies. This proviso is not merely a shield to hide under: the problems involved in making adequately controlled measurements of this kind on living cells under physiological conditions are formidable. The ideal approach would be to measure the force of adhesion directly (i.e. by mechanical means) as a function of separation distance (i.e. over a range of perhaps 10–1,000 Å) for surfaces of simple geometry and area. In 1956 Derjaguin et al. measured electrodynamic forces between macroscopic quartz bodies in a vacuum, providing the first experimental verification of Lifshitz's theoretical method (Lifshitz, 1956). In this experiment all the criteria listed above were met. But to do a similar experiment with cells is much harder. Water greatly curtails the range of physical interaction; this entails measuring smaller separation distances. One has also to deal simultaneously with electrostatics due to the interaction of double layers at cell surfaces as well as with electrodynamics. Cells do not generally have well defined shapes: they deform when pulled apart and measurement of the small area of contact is an additional problem. Furthermore, cells live in a medium containing complex macromolecules which adsorb on any "clean" surface which may be used to assess adhesion. Even washed cells can lose macromolecular materials which may contaminate a clean surface.

The simplest way to look at the physics of cell adhesion is to forego the luxury both of physiological media and living cells. Glutaraldehyde fixation helps to prevent loss of proteins and glycoproteins from the cell surface into simple salt solutions. Furthermore, fixation increases cell rigidity, thereby tending to stabilize the area of contact with little change in the electrostatic charge on the cell (Vassar et al., 1972; Todd and Gingell, in preparation) or the distribution of the charge-carrying glycoproteins in the lipid bilayer (Pinto da Silva, 1972). Human red blood cells were used because of their relatively simple shape and because more is known about the molecular architecture of their surface membrane than any other type. It may be objected that we are perverse in choosing to investigate the adhesiveness of a cell which is, perhaps above all other metazoan cells, designed to be nonadhesive. This, however, could be construed as a good reason for investigating the magnitude of physical forces in the system; if significant attractions are found here they should be at least as big elsewhere. We also decided that more information would be extracted from the interaction of cells with an inert substratum than interaction with other cells. A substratum offers several advantages: one can choose a substratum of which the electrodynamic and electrostatic parameters can be determined; on certain metals the electrostatic charge density can be varied continuously, and surfaces can be made which are probably molecularly smooth. Further, the interaction between a "known" body and an "unknown" offers more hope for analysis than interaction between two "unknowns" in terms of the

physical properties of the surfaces. Nevertheless, we fully appreciate that a full understanding of intercellular adhesion can only be attained from studying how cells stick to *cells*.

Previous experiments on the adhesion of red cells to an oil-water interface, charged by ionized detergents (Gingell and Todd, 1975) have shown that adhesion to the interface is total when the ionized charge is zero or positive, but that adhesion can be prevented by electrostatic repulsion when the interfacial charge is made sufficiently negative. We were thus able to demonstrate an attractive force, possibly of electrodynamic origin, underlying the electrostatics. Since it is hard to measure the charge density with any confidence under our experimental conditions, we have since developed a different method where an interfacial charge density can be accurately determined.

The technique we have used is to assess the adhesion of glutaraldehyde-fixed human red blood cells to a smooth polarizable lead electrode in dilute sodium fluoride solution. The charge density on such an electrode can be determined with precision by measuring electrode capacitance. In sodium fluoride, analysis of the results is facilitated because neither sodium nor fluoride ions adsorb to lead over its wide range of polarizability. Adhesion of cells to the electrode is assessed by allowing adequate settling time and then inverting the continually polarized electrode. If cells are non-adherent they fall off. This method allows us to define a "critical" charge density and consequently an electric surface potential on the electrode at which cells just fail to adhere to the metal. At this point the force of adhesion is equal to the electrostatic force of repulsion. Knowing the ionic strength, the charge on the metal and on the red cell, the repulsive force can be calculated.

METHODS

Materials and Reagents

Water, twice distilled in glass, was redistilled from alkaline potassium permanganate and again from orthophosphoric acid in an all-glass apparatus. Its surface tension at 25°C was 73.0 dyn/cm which corresponds almost exactly with the value obtained at the Unilever Research Laboratory at Port Sunlight (J. Mingins, personal communication), but is slightly higher than the value of 71.97 given in the *Handbook of Chemistry and Physics* (1974).

Glassware which had not been used exclusively for "clean" work was first treated with cold chromic acid, rinsed in two times distilled water, then immersed for a few minutes in a mixture of 4% by volume Analar hydrofluoric acid and 50% by volume Analar nitric acid in two times distilled water (BDH Chemicals Ltd, Poole, Dorset, England). The chromic acid treatment was omitted for routinely used glassware. Great care is necessary in handling the hydrofluoric acid mixture (Mingins and Taylor, 1974). The glassware was then rinsed thoroughly in four times (best) distilled water, dried in air and kept in a dust-proof cabinet if not used immediately. The hydrofluoric acid solution etches glass slightly and therefore small volume volumetric glassware was not exposed to it.

Plastic components were sonicated in Analar methanol then Analar diethyl ether and dried in air for several hours after solvents could be smelt. After this procedure the assembled plastic electrode chamber was filled with the working solution for one or two days and then emptied before final filling as a precaution against traces of water-soluble impurities. In routine use it was simply flushed with electrolyte.

Sodium fluoride was obtained 6× recrystallized (Koch-Light Laboratories Ltd., Colnbrook, Buckinghamshire). This was roasted in a muffle furnace at 800°C for 10 h in a platinum crucible to oxidize any traces of organic matter which might otherwise adsorb to the lead electrode.

Human red cells obtained by venipuncture were washed four times by centrifugation in normal saline then fixed in 3.3% glutaraldehyde in normal saline at 4°C for 18 h. The cells were then washed exhaustively in 0.001 M NaF by centrifugation and suspended in 0.001 M NaF.

Circuit

A Wayne Kerr B221 capacitance/resistance bridge (Wayne Kerr Lab Ltd., Bognor Regis, Sussex) was used to measure the capacitance of the lead electrode. The later model B224 is far less sensitive and is completely unsuitable for electrochemical work. The internal oscillator was supplanted by an external Marconi wide-range oscillator, model TF1370A (Marconi Instruments Ltd., St. Albans, Hertfordshire), with variably attenuated sine wave output. This fed into the bridge through an isolating transformer to avoid earthing the bridge through the oscillator (Fig. 1). In later experiments a battery-operated Levell oscillator, model TG200DM (Levell Electronics Ltd., High Barnet, Hertfordshire) calibrated against a frequency counter was used. A tunable STC null detector, model 96016 (Standard Telephones and Cables Ltd., Newport, Monmouthshire), embodying a high gain amplifier with microvolt sensitivity was used to find the balance conditions of the bridge. One 6 V dry cell supplied a Beckman LP10 precision Helipot potentiometer (Beckman Instruments, Inc., Schiller Park, Ill.) from which polarizing potential was applied between the working (lead) and counter (platinum) electrodes. A 70 Henry choke blocked alternating current from the DC polarizing circuit, while paper capacitors in parallel totaling 1,000 μF were used to prevent direct current from flowing through the bridge. The circuit was tested using a Sullivan C1855 0.01 μF standard (Sullivan Ltd., Dover, Kent) in place of the working and counter electrodes and it was ascertained that the DC polarization system did not disturb the balance of the bridge. Further circuit tests are described in Appendix B. The potential of the working electrode with respect to a miniature calomel electrode was measured using a Corning EEL digital millivoltmeter (model 109; Corning Scientific Instruments, Medfield, Mass.) with input impedance in excess of 10^{13} Ω. This instrument was switched out of circuit while balancing the bridge, in order to avoid capacitance error. The calomel electrode
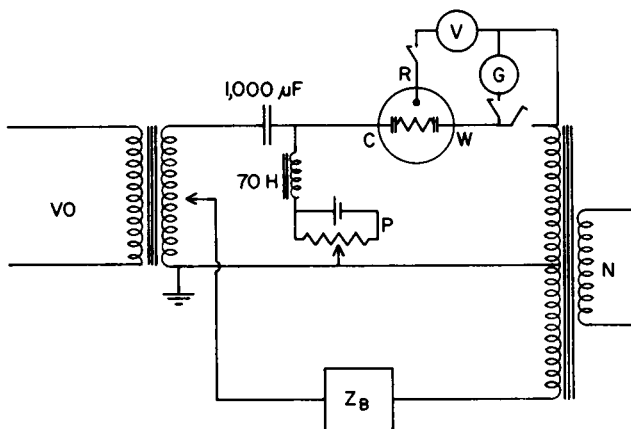

FIGURE 1 Circuit for measuring capacitance of the polarized electrode. V, high impedance voltmeter; G, moving spot galvanometer; VO, variable oscillator; N, null detector; R, calomel reference electrode; W, working polarizable lead electrode; C, platinum counter electrode; Z_B, bridge impedance standards; P, potentiometer.

was interfaced with saturated potassium chloride whose diffusion into the electrode chamber was restricted by a short plug of stiff agar. Care was taken to ensure that the measuring signal experienced by the working electrode did not exceed 18 mV peak-to-peak.

Early experiments were carried out in an open room, but better electrical behavior was obtained later in a Faraday cage.

Working Electrode Encapsulation

The electrode was made from Koch-Light 99.9999% pure lead wire of 3 mm diam. A length of about 2 cm was soldered to a brass rod 0.2 cm diam × 5 cm long. The brass rod was held in a lathe chuck and the lead was turned to 0.250 cm then very briefly chemically polished and dried in warm air. The electrode was then held by the brass rod, to prevent the soft lead being damaged by contact with solid surfaces, and washed in alcohol, then ether and air dried. Two-part ultra-pure epoxy resin OSO100 (Hysol-Sterling Ltd., London), designed for the encapsulation of solid-state electronics, was warmed at 60°C for several hours to dissolve the crystals which normally appear at room temperature, and the two parts were mixed accurately in the manufacturers' recommended proportions by weight. The viscous resin was poured into a three-part polytetrafluoroethylene (PTFE) mold (previously cleaned by sonicating in alcohol then diethyl ether and dried) and degassed at 40 torr at room temperature. When air bubbles ceased to be given off, the lead electrode was inserted axially in the resin and a PTFE cap put on to maintain axiality of the electrode. The resin was degassed again and then put in an oven at atmospheric pressure for 20 h at 120°C to cure. Degassing is a troublesome procedure and complete removal of air is difficult. The resin does not adhere to PTFE and is easily removed from the mold. Since the resin sets optically transparent and colorless, the lead plug could be easily examined—it remained brilliant and uncorroded. The resin apparently adheres to the lead and does not split away on cooling from 120°C to 20°C. No creep of water or alcohol, which would indicate an annular gap between lead and resin (a serious defect) was seen under a Zeiss binocular dissecting microscope (Carl Zeiss, Ltd., London). In contrast, solvent "creep" was observed even after making nominally good interference fits in Kel-F (Fluorocarbon Ltd., Hertford, Hertfordshire) or PTFE, both of which proved to be completely unsatisfactory encapsulating materials. The diameter of the lead face in the completed electrode was checked using a micrometer eyepiece in a low power microscope.

Cutting the Working Electrode

We found that it was possible to surface a lead electrode using a Cambridge ultramicrotome (Cambridge Instrument Co., Ossining, N. Y.) with a glass knife. A modified chuck was made to hold the encapsulated electrode, but otherwise the instrument was standard. After rough facing on a lathe, followed by sonication in methanol to remove traces of mineral oil, the electrode was placed in the clean chuck and cut in 1 μM increments until a smooth, flat, reflective surface had been obtained. Larger advances sometimes caused the hard encapsulating resin to chip and chatter. It is absolutely essential that abrasives should not be used to face the electrode prior to cutting, otherwise carborundum particles embedded in the lead surface ruin the glass knife, embedding fragments of glass in the lead and rendering it impossible to cut sections without scratches, however many times the knife is changed. The surface of the lead electrode after dry cutting is quite distinct from chemically polished lead; the individual crystals are plainly visible to the naked eye. That this is evidence of crystalline structure rather than partial oxidation is shown by the constancy of the pattern over a large number of sections. After the dry cutting process the lead surface appears to remain unoxidized in dry air for several hours, though if cut under water oxidation is evident in less than a minute. We found that a smoother surface could be obtained by lubricating the electrode with spectroscopically pure hexadecane during cutting, then sonicating for a few seconds in Analar ether, methanol, and then best distilled water. Less

than 15 s elapsed before the electrode was then placed under polarization in the chamber. Electrodes cut, but not chemically polished, gave capacitance curves similar to those cut and polished, and were on the whole more stable and were far easier to prepare. The results reported here were obtained with electrodes prepared by both methods.

Chemically Polishing the Working Electrode

The working surface of the encapsulated lead electrode was polished by a modification of Grifkins's (1961) method: a mixture of 30 parts by volume of 100 vol Analar hydrogen peroxide, and 20 parts by volume of Analar glacial acetic acid was made up to 100 parts by volume with Analar methanol. 50 ml of the freshly made mixture was poured rapidly across the working face of the horizontally held electrode while it was rotated to avoid streaks; the electrode was then agitated for a few seconds in methanol. The procedure was repeated using the same polishing solution, until a smooth, brilliantly lustrous surface had been obtained. The electrode was then washed vigorously in a jet of distilled water to remove all traces of polishing solution. Polishing was continued if the surface looked even slightly milky (oxidized) under a 15 W microscope light source. Even good overhead lighting can fail to show up serious oxidation at this stage. When a satisfactory polish had been achieved the electrode was inserted into the chamber within 10 s; while the electrode is wet and exposed to air, speed is vital. This procedure is more art than science and requires a great deal of practice to achieve even moderate consistency.

Electrode Chamber

The electrode chamber was constructed from a 3-in diam rod of polychlorotrifluoroethylene, Kel-F, specially molded by Fluorocarbon Ltd. This was made without plasticisers and has chemical inertness similar to the more familiar polytetrafluoroethylene (PTFE). However, it has the distinct advantage over PTFE of a constant coefficient of expansion around room temperature, and is thus more suitable for precision components. The lid of the chamber (Fig. 2) has a round glass coverslip window (22 mm diam) held in position by a top hat-shaped retainer into which the microscope objective can move. Three stainless steel screws secure the retainer to the lid, and six more hold the lid to the base. Attached to the chamber lid with Kel-F screws is a collar into which the working electrode is seated. A hole, 2.5 mm diam, was drilled through the collar in the optic axis. The working surface of the lead electrode is viewed down this hole, at a depth of approximately 6 mm below the coverslip, using a specially built epi-illumination microscope with Zeiss long working distance UD40 objective, the system having an overall linear magnification of 250. Running across the hole, immediately below the coverslip, is a 1 cm wide transverse slot communicating with the bulk electrolyte. Into this slot projects the needle of the Hamilton syringe used for introducing cells. When positioned, the orifice of the syringe is 2 mm vertically above the center of the lead electrode. The syringe runs in a guide in the chamber wall which incorporates a silicone rubber diaphragm which is penetrated by the needle. The counter electrode is a 4 cm diam platinized platinum disc welded to a platinum wire which runs through a silicone rubber seal compressed by a brass terminal screwed to the lid. A pair of concentric stainless steel screws compress a PTFE 'O' ring around the working electrode, holding it securely in place. Release from compression by loosening the inner screw allows the electrode to be rapidly withdrawn and replaced—a device similar to certain high vacuum seals.

The Microscope

An epi-illumination microscope was built on a hinged platform so that it could be used upright, upside-down, or at intermediate angles. Viewing is facilitated by a right angle head piece which obviated the necessity for contortions when the microscope was inverted. The Zeiss UD 40 objective gave a sufficient working depth for focusing on the working surface of the lead electrode in the chamber. Initially, the microscope was screwed to a bench, but artefactual cell detach-
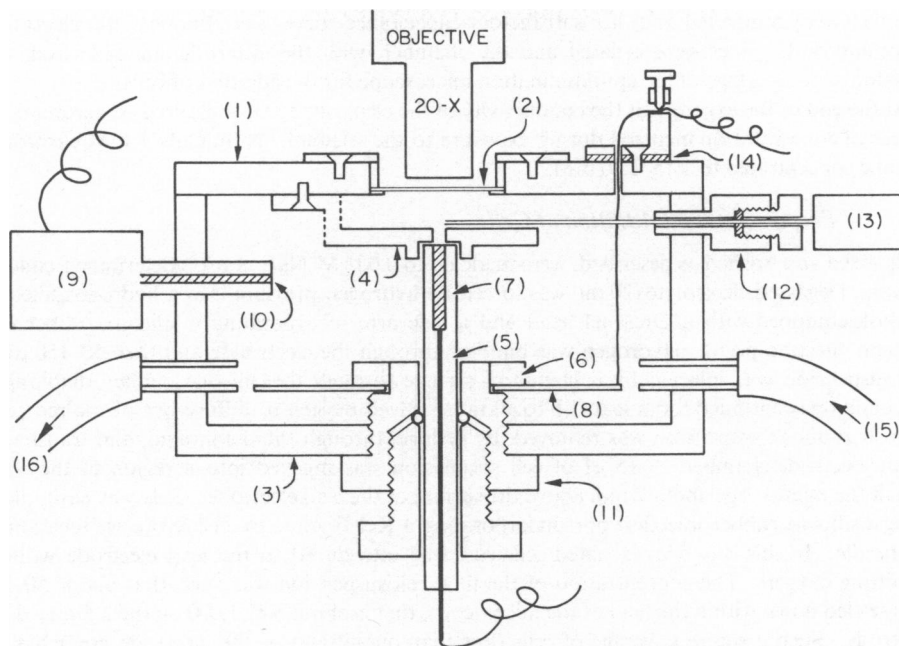
FIGURE 2   Electrode chamber. 1, lid; 2, glass window; 3, base of chamber; 4, collar receiving working electrode; 5, resin encapsulated working electrode; 6, counter electrode clamping ring; 7, lead electrode; 8, platinized platinum counter electrode; 9, calomel reference electrode; 10, agar plug; 11, seal for working electrode insertion; 12, silicone rubber seal for hypodermic needle insertion; 13, glass syringe for cell injection; 14, silicone rubber seal for counter electrode wire; 15 and 16, inlet/outlet for hydrogen/electrolyte.

ment due to vibration (a Bach organ prelude, on one occasion) caused us to mount it on a half-ton steel base.

Degassing the Electrolyte and Filling the Chamber

There is no stage in the preparation of a polarizable lead electrode more critical than rigorous deoxygenation of the electrolyte since in the presence of water and oxygen the corrosion of lead is very rapid. We found vacuum degassing of the electrolyte to be completely inadequate and decided to resort to the more complicated procedure of freezing and thawing in a vacuum, rather than the less certain method of bubbling hydrogen or nitrogen. On freezing, gas cannot be incorporated in the crystal structure of ice and is expelled as bubbles which are released as the ice melts. After three such cycles, the electrolyte vessel was brought to atmospheric pressure with hydrogen and could be left for a day or so at a small excess pressure without noticeable re-oxygenation. The electrolyte was then forced by hydrogen pressure into the chamber through a pipeline of glass with silicone rubber joints. Both pipeline and chamber were thoroughly purged with hydrogen slightly above atmospheric pressure immediately prior to the passage of degassed electrolyte.

The chamber was filled with electrolyte using a stainless steel plug in place of the working electrode. When the electrode was prepared it was rapidly inserted in place of the steel plug. Oxygen that entered the chamber at this stage was immediately purged with hydrogen and then the chamber was finally topped up with electrolyte. At this stage the electrical connections to the

chamber were completed and, if a satisfactory capacitance curve was obtained, the electrolyte input and outlet pipes were isolated and the chamber, with the electrode still polarized, was transferred to the stage of the epi-illumination microscope for the addition of cells.

At the end of the experiment the conductivity of the electrolyte was measured to ascertain the degree of concentration incurred during exposure to the vacuum. Nominally 1 mM electrolyte became concentrated to 1.15–1.20 mM.

Preparation and Addition of Cells

Cells, fixed and washed as described, were made up to 0.001 M NaF at a predetermined concentration. Degassed electrolyte (20 ml) was forced by hydrogen pressure into a hydrogen-filled 50 ml flask equipped with a Dreschel head and a side arm incorporating a silicone rubber diaphragm injection point. Hydrogen was bubbled through the electrolyte and then 50–150 μl of cell suspension was injected by a Hamilton syringe through the silicone rubber diaphragm. Bubbling was continued for at least 1 h to allow dissolved oxygen to diffuse out of the red cells, then 20 μl of cell suspension was removed, by syringe, through the diaphragm, and transferred to the electrode chamber. 5–15 μl of cell suspension was injected into a region in the optic axis of the microscope about 2 mm above the surface of the lead electrode. This was easily done using a silicone rubber injection port incorporating a Kel-F guide to ensure precise location of the needle. In this way deoxygenated cells could be introduced to the lead electrode without admitting oxygen. The concentration of the final cell suspension was such that about 50–100 cells settled down within the field of the microscope, that is about 500–1,000 on the 2.5 mm diam electrode. Such a sparse coverage of cells (less than one-fiftieth of the electrode area) has no measurable affect on the capacity of the electrode. The polarizing potential remained constant ($\pm$ 1 mV) during addition and subsequent viewing of the cells which sometimes extended over several hours.

The rather complicated rigmarole described was the result of a great deal of experimentation and initial failure. Small details can be vital and we would be happy to advise anyone attempting to set up a similar system for biological or chemical work.

THEORY OF THE METHOD

A remarkable achievement in surface chemistry due to Grahame (1947, 1954, 1957) was the development of an accurate method for measuring the surface charge density of a mercury electrode immersed in an aqueous salt solution. The mercury interface is *polarizable,* this is, it has a very high DC resistance and consequently leaks only a very small current when charged by a potential difference applied across it. When charged in this way the metal surface acts as one plate of a capacitor, inducing a space charge of equal magnitude, but opposite sign (diffuse double layer) in the nearby electrolyte. The extent of this charge, which constitutes the second "plate" of a molecular capacitor, depends on ionic strength. It is about 10 Å in 0.1 M NaCl and about 33 Å in 0.01 M NaCl. Grahame, and subsequently others, used a Wheatstone bridge circuit to measure the differential capacitance of the electrical double layer at the surface of falling mercury drops as a function of the applied DC polarizing potential difference. From the measured capacitance it is possible to calculate the surface charge on the metal at any given applied polarizing potential. More recently, Rybalka and Leikis (1966) used a similar method to determine the surface charge on a lead electrode.

Capacitance is defined as $C = q/\Delta\phi$, where $\pm q$ is the charge on the plates and $\Delta\phi$

is the Galvani potential difference across the capacitor. But in an electrical double layer, capacity is a function of surface charge density. Thus it is necessary to define a differential capacitance $C(q)$.

$$C(q) = dq/d\Delta\phi. \tag{1}$$

$\Delta\phi$ is the Galvani potential difference between the bulk phases of the material of the electrode (metal) and the abutting solution (electrolyte). Capacitance here will always mean differential capacitance and will be simply written C. Integration of differential capacitance with respect to potential gives charge

$$\int_{q(\Delta\phi_1)}^{q(\Delta\phi_2)} dq = \int_{\Delta\phi_1}^{\Delta\phi_2} C\, d\,\Delta\phi. \tag{2}$$

If the conditions under which $q(\Delta\phi_1) = 0$ are known, the electrode charge can be found. Then

$$q_m = \int_{\Delta\phi_1(q_m=0)}^{\Delta\phi_2} C\, d\Delta\phi. \tag{3}$$

Since the reference calomel electrode is reversible, any change in potential $\Delta\phi$ between reference and working electrodes due to an impressed voltage occurs entirely across the polarizable working electrode. The potential of zero charge $\Delta\phi_1(q_m = 0)$, or pzc, can then be measured as the polarizing potential difference ΔV between working and reference electrodes when $q_m = 0$. The pzc for liquid mercury can be thermodynamically identified with the potential corresponding to the electrocapillary maximum (Grahame, 1947). Electrocapillary methods cannot, of course, be applied to solids but alternative procedures are available (see Perkins and Anderson, 1969). For example, in sufficiently dilute electrolyte there is a sharp minimum in the capacitance at the pzc. This minimum is due to the diffuse region of the electrical double layer and is predicted by the Gouy-Chapman equation (Grahame, 1947). It is common practice to refer potentials to the pzc, defining a rational potential scale where $V_{pzc} = 0$.

All the necessary information is, therefore, available for the evaluation of Eq. 3 giving the charge on the working electrode. Note that this argument makes no assumption that $\Delta\phi_1 = 0$ at the pzc: it only says that a potential difference between working and reference electrodes can be found such that there exists some $\Delta\phi_1$, for which q_m is zero.

Differential capacitance of the working electrode conveniently measured using a transformer ratio-arm capacitance/resistance (CR) bridge (Bockris et al., 1966). The Wayne Kerr B221 bridge employs standard capacitors and resistances in parallel which are balanced against the unknown impedance. This consists of the working electrode, working electrolytic solution and platinum counter electrode. Since these elements are connected in series the large value of the counter electrode capacity C_c makes a negligible contribution to the total capacity C_T, which is then equal to the capacity of the working electrode C_w

$$1/C_T = (1/C_c) + (1/C_w). \tag{4}$$

Since $C_c \gg C_w$, $C_w = C_T$ to within any desired accuracy. Sufficiency of C_c was assessed by increasing counter electrode area: no change in C_T resulted. The sinusoidal signal from the oscillator was kept low (18 mV or less, peak to peak, though higher voltages can probably be used safely except near the *pzc*) in order not to unduly perturb the double layer at the working electrode face. If the signal is large enough to significantly affect q_m in regions where C_w changes rapidly with q_m the differential capacitance becomes a function of signal amplitude.

Capacitance of the working electrode C_w and combined resistance of the working and counter electrodes R_E in series are related to the equivalent capacity C_B and resistance R_B in parallel in the bridge at balance by the relations.

$$C_w = C_B(1 + \alpha^2)/\alpha^2, \tag{5}$$

$$R_E = R_B/(1 + \alpha^2), \tag{6}$$

where $\alpha = 2\pi f C_B/R_B$, f being frequency in Hz. There should be little or no frequency dependence if the geometry of the working and counter electrodes assembly can be optimized (Grahame, 1946), but in the cell chamber this was not achieved (Appendix B) and we were consequently obliged to make our measurements at low frequency, 208 Hz.

RESULTS

Capacitance Measurements

As soon as the working electrode was introduced into the chamber its rest potential with respect to the calomel reference electrode was measured. This did not turn out to be a reliable guide to good capacitance behavior; nearly all electrodes gave resting potentials in the region of -530 to -600 mV in 0.0012 M NaF. Care was taken to adjust the potentiometer before connecting the working electrode in the polarizing circuit to ensure that the electrode did not experience a less negative potential than this, since we noticed that irreversible changes (probably corrosion of the lead) can occur at polarizing potentials lower than the resting potential where the electrode is strongly positively charged—since the *pzc* is -840 mV.

Rybalka and Leikis (1966) recommended that the lead electrode should remain polarized for an hour at a potential corresponding to $-1,380$ mV with respect to a calomel electrode. This procedure did not improve performance in our hands; bad electrodes stayed bad and usually got worse. Nor did the ritual of cycling the potential several times through the range -700 mV to $-1,700$ mV, to remove adsorbants from the working surface of the lead electrode, have any effect. At potentials more negative than $-1,800$ mV the hydrogen overvoltage is exceeded and H_2 gas is evolved. Capacitance curves were obtained over the polarization range -700 to $-1,700$ mV. Results are shown in Fig. 3, together with results of Rybalka and Leikis (1966) and of Grigor'ev and Machavariani (1970) for comparison. When a good curve was ob-
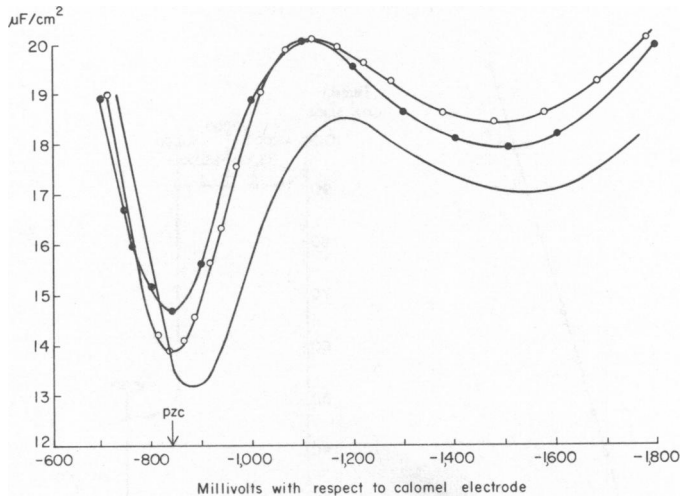
FIGURE 3 A Capacitance curves for lead in NaF solution. ●, Our result: 0.012 M NaF (208 Hz).
○, Rybalka and Leikis (1966): 0.010 M NaF. ——, Grigor'ev and Machavariani (1970): 0.010 M
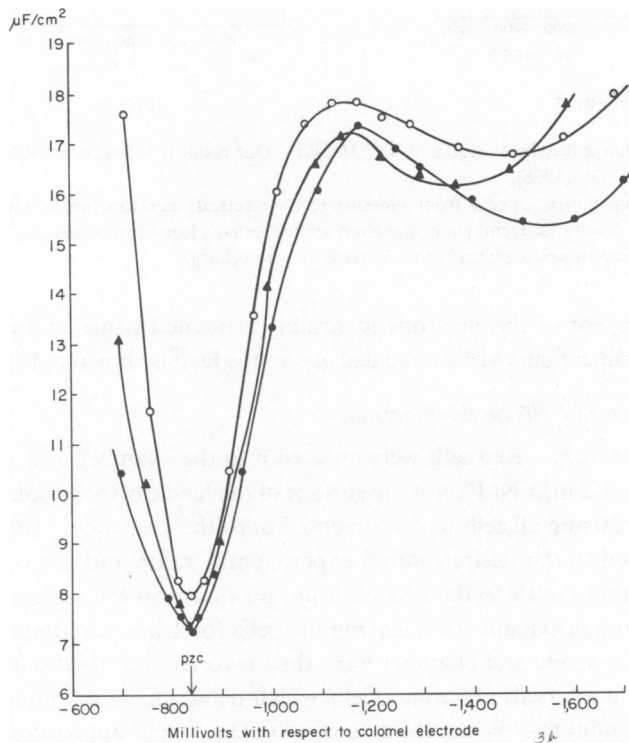NaF. The potential of zero charge is shown as *pzc*.

FIGURE 3 B Capacitance curves for lead in dilute NaF solution. ●, Our result: 0.0012 M NaF,
208 Hz, and ▲, 40 Hz. ○, Rybalka and Leikis (1966): 0.001 M NaF. The potential of zero charge
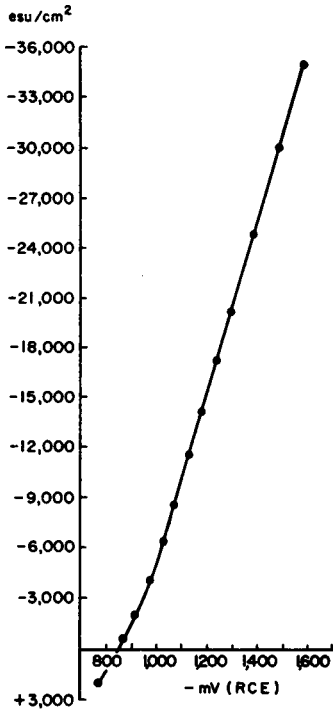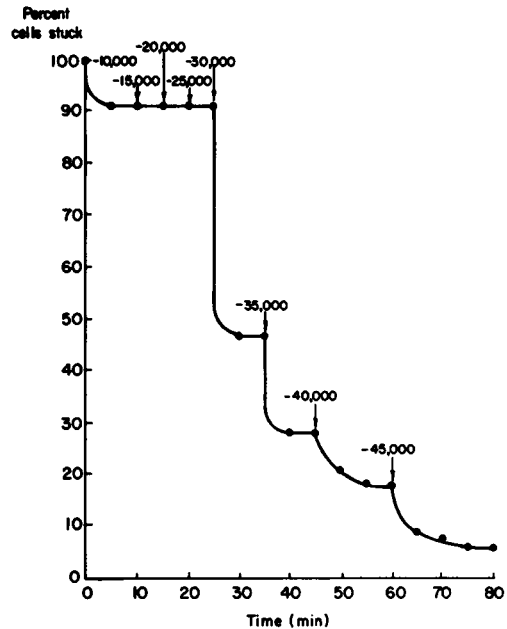is shown as *pzc*.

FIGURE 4

FIGURE 5

FIGURE 4   Charge density on lead in 0.0012 M NaF. Our result is indistinguishable from that of Rybalka and Leikis (1966).

FIGURE 5   Detachment of cells from adhesion to the electrode as a function of time. The times where charge density (esu/cm^2) was increased are indicated. Equilibrium percent of cells stuck is given by the appropriate plateau of the curve for a given charge.

tained, the behavior of the electrode invariably remained constant for several hours. The practically linear curve of charge density on the lead is shown in Fig. 4.

Behavior of Cells on the Electrode

1.2 mM NaF.   Red cells were injected into the chamber and allowed to settle under gravity in 1.2 mM NaF onto the surface of the lead electrode polarized at $-3,500$ esu/cm^2. After 20 min all cells had sedimented onto the electrode. The charge density was then reduced to the desired initial experimental value and the cells were left an additional 20 min to settle to their equilibrium positions on the surface. (That 20 min is sufficiently long is evident from leaving the cells for 1 h and obtaining identical results.) The microscope and chamber were then inverted and the fraction of adherent cells was noted at intervals of 5 min. Cells which detach from the interface usually do so within a few minutes. When the rate of cell detachment approached zero the electrode charge density was increased to a more negative value and the detachment process was again observed. This sequence of events was continued until a maximum electrode surface charge density of $-45,000$ esu/cm^2 was reached (Fig. 5). At charge
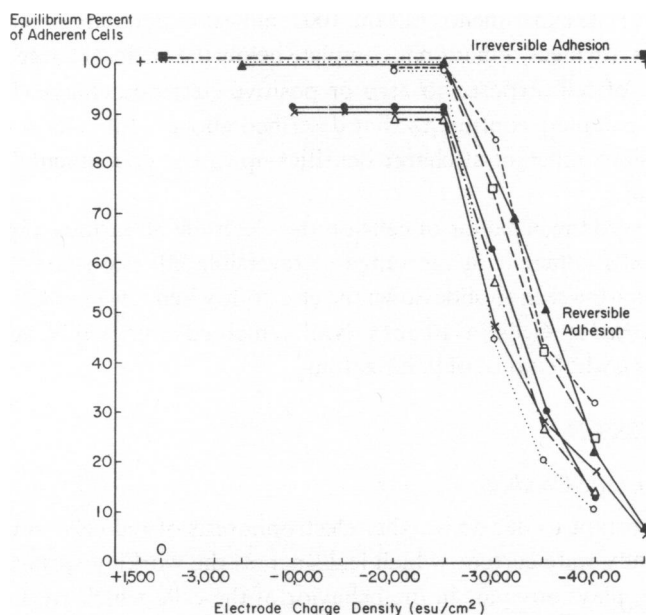
FIGURE 6 Equilibrium percentages of cells adherent to the electrode as a function of surface charge density. Each point is taken from plateau data of the type shown in the previous figure. Single lines which remain constant at 100% for cells starting at zero and positive values of surface charge represent half a dozen identical results.

densities of $-25,000$ esu/cm^2 or less,[1] 90–100% of the cells remained adherent to the electrode; Fig. 6 shows the results of several such experiments. However, cells which had not been exposed to a very low electrode charge (near the point of zero charge) showed an abrupt change in behavior on moving to higher charges; some lost their face-on adhesion and remained attached to the surface by their edge, remaining thus indefinitely if the charge was not altered, while other cells could be seen sedimenting away from the surface, usually falling edge on. We adopted the criterion of counting cells as adherent if they were face on but not if they were edge on. This applied to cells which had settled before inversion, as well as afterwards. At $-30,000$ esu/cm^2 about 60% of the cells remained adherent and at $-35,000$ esu/cm^2 30% remained; about 10% could not be removed at the maximum obtainable polarization of $-45,000$ esu/cm^2. A constant feature of all these experiments must be emphasized: after the initial inversion at polarizations in the range $-5,000$ to $-25,000$ esu/cm^2 where between 0–10% of the cells fell off, no further loss of cells occurred until the charge was increased from $-25,000$ to $-30,000$ esu/cm^2. When this happened, cells always fell off. It is therefore apparent that between $-25,000$ and $-30,000$ esu/cm^2 is a critical region for cell adhesion and $-25,000$ esu/cm^2 will be referred to as the critical charge. We do not know why a few cells sometimes fell off upon initial inversion at charges less than the critical

---

[1] More and less refer to the magnitudes of the negative charge densities.

charge in some of the experiments, but the 100% adhesion frequently seen suggests that when conditions are ideal, adhesion is complete below the critical charge density.

The behavior of cells exposed to zero or positive electrode charge, for even a few minutes was in complete contrast to that described above. All cells subsequently remained irreversibly adherent at charge densities up to the experimental maximum of $-45,000$ esu/cm^2.

We also observed the behavior of cells on the electrode at various angles of inclination. Neither cells adherent in the range of reversible adhesion nor those in the irreversible region were seen to slide down the electrode when it was at 45° or 90°.

10mM NaF. Cells in 10 mM NaF remained immovably adherent to the electrode over the whole range of polarization.

DISCUSSION

Electrostatic Conditions

It is clearly important to decide whether electrophoresis of red cells in the field set up by the small steady-state current, which leaks across the working surface of the polarizable electrode, plays any part in the behavior of the cells which we have described. For example, is cell detachment really electrostatic, or could it be electrophoretic— or even a combination of the two?

A galvanometer placed in series with the working electrode (Fig. 1) indicated a current of 0.116 μA (2.56 μA/cm^2) at a polarization of $-30,000$ esu/cm^2 which is increased to 0.192 μA (4.24 μA/cm^2) at $-45,000$ esu/cm^2 (Fig. 7). Such nonlinear current voltage characteristics are normal, and are described by the Butler-Volmer equation (Bockris and Reddy, 1973). We ascertained that no surge of current, in excess of the steady-state leakage value plus the tiny current to charge the working electrode, occurred when the polarization was changed rapidly by several hundred millivolts. During normal operation of the polarization circuit, current is drawn to charge the 1,000 μF blocking capacitor as well as the working electrode: these currents were measured by placing the galvanometer in appropriate parts of the circuit. This check was made to ensure that cells were not exposed to electrophoretic currents higher than steady values during the process of changing the polarization.

The field experienced by the cells is readily calculated from this current. The dimensions of the electrolyte-filled cylindrical hole in the plastic collar, which the working electrode faces, were chosen such that the current density over the whole electrode surface is uniform (Powers, 1967); consequently the electric field within the collar is also uniform both in cross section and longitudinally. By Ohm's law, the field in the axis of the cylinder is $E = \rho I/A$, where ρ is the specific resistance of the electrolyte (10^4 Ω cm), I is the current, and A is the area of cross section of the cylinder. Thus $E = 4.24 \times 10^{-2}$ V/cm at $-45,000$ esu/cm^2. We measured the electrophoretic mobility of the experimental cells in a Zeiss cytopherometer at 20°C and found it to be 6.6 μm/s/V/cm in the working electrolyte. The steady-state electrophoretic velocity of cells within the collar at maximum polarization must therefore be $4.24 \times 10^{-2} \times$
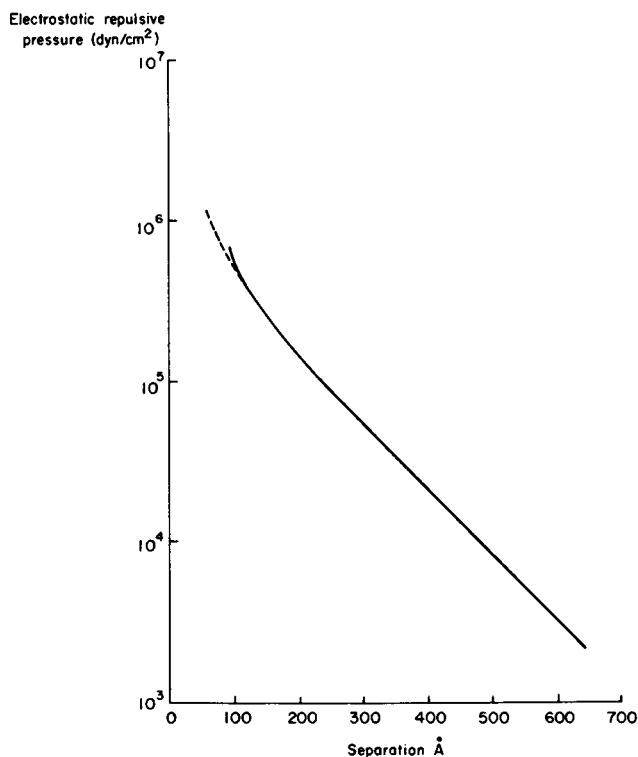
FIGURE 7 "Critical" electrostatic pressure just sufficient to prevent cell adhesion in 1 mM salt solution as a function of distance from a polarized electrode. The electrode charge density from our experimental data is $-25{,}000$ esu/cm^2 and the cell surface charge density is taken as $-5{,}000$ esu/cm^2. Nonlinear solutions: solid curve, constant surface charge model; broken curve, constant surface potential model.

$6.6 = 0.28 \, \mu\text{m/s}$. With this information it is easy to make a direct comparison between electrophoretic and gravitational forces. Consider a cell freely suspended in electrolyte within the horizontally oriented collar: the electric and gravitational fields are mutually perpendicular. The equilibrium velocities in these directions are proportional to the electric and gravitational forces, the proportionality constant being Stokes drag (observation shows that this is independent of cell orientation for both sedimentation and electrophoresis). Since the sedimentation velocity under gravity was found to be 2 μm/s, gravity exceeds the electrophoretic force by a factor of $2/0.28 = 7$ at maximum polarization, where the electrophoretic effect is greatest. At a polarization of $-30{,}000$ esu/cm^2, where cells are beginning to detach from the electrode, the factor is 12. These calculations show that the maximum electrophoretic force is considerably smaller than gravity; indeed, it must be smaller, otherwise cells could never sediment downwards onto the surface of a negatively polarized electrode.

Release of cells from reversible adhesion to the electrode will occur when the difference between attractive and repulsive forces is equal to the gravitational force plus

the electrophoretic force $\mathcal{E}$ which acts in the same direction as gravity when the microscope is inverted.

$$|F_A| - |F_R| = mg + \mathcal{E}.$$

Since $\mathcal{E} \ll mg$ we will neglect the electrophoretic term and write

$$|F_A| - |F_R| = mg.$$

The experiment is adequately electrostatic for our purposes.

Primary and Secondary Minima

As Curtis (1962) pointed out, the classical theory of colloid stability (DLVO theory) predicts that two distinct kinds of adhesion can occur. At some finite separation, interacting bodies can reach an equilibrium where electrodynamic attractive and electrostatic repulsive forces are equal and the potential energy of interaction is a local minimum; this is the secondary minimum configuration. At all larger distances the net force is attractive—so there is no net energy barrier for bodies entering the secondary minimum from larger separations. But at distances less than the secondary minimum there is a net energy barrier to closer approach. Both the height of this barrier and the depth (stability) of the secondary minimum depend on ionic strength and electrostatic charge. At the smallest separation (limit of close approach) the theory, which is rather unreliable in this region, predicts a deep energy well or primary minimum. More sophisticated calculations underline the apparent applicability of these concepts to the interaction of cells with other cells and with inert substrata.

Since the ionic strength of the medium and charge density on the metal surface can be varied in our experimental system to produce a very wide range of electrostatic repulsion, we anticipated that if secondary minima can exist for the interaction of a cell with a surface we should be able to find the appropriate conditions for it. We think that this may have been achieved for the following reasons:

(1) Almost 100% of the cells adhere reversibly to the electrode in 1.2 mM NaF if they are allowed to settle onto it within a wide range polarization charge from near zero to $-25,000$ esu/cm^2. A reversible adhesion over a range of surface charge is predicted for secondary minimum adhesion.

(2) If the negative polarization of the inverted electrode is increased to $-30,000$ esu/cm^2 or more the reversibility of adhesion becomes apparent as the cells begin to fall off. By $-45,000$ esu/cm^2 about 90% have lost their adhesion.

(3) Between near zero charge and $-25,000$ esu/cm^2 virtually all the cells are stably adherent to the electrode and do not slowly sediment off. The cells are therefore not retained by viscous forces. This behavior is expected in the secondary minimum, since increasing the charge forces the cells further away from the surface, progressively lessens the depth of the potential energy well and reduces the force required to escape from it, until at a critical repulsion the force of gravity is sufficient to pull the cells out of the potential well. This is precisely the behavior we have described. Neverthe-

less the only way of proving that a secondary minimum exists is to measure the aqueous gap between cell and surface.

We feel confident that primary minimum adhesion has been demonstrated, since a sufficient reduction in the negative charge on the electrode, to near zero or to positive values, causes irreversible adhesion. Cells cannot then be "blown off" by increasing the negative potential—adhesion is 100% even at maximum negative polarization.

An explanation is required for our inability to detect cell sliding under conditions where we expect there to be secondary minimum adhesion, since cells in a secondary minimum should be free to slide in the plane of the surface (Gingell, 1971). Our observational technique should have enabled us to detect a movement of about 2 μm, yet over a period of 1 h no movement was detected on either cut or chemically polished electrodes which were oriented so that the plane of the interface was vertical. Assuming contact area of 1 μm^2, a viscosity of 0.01 P, characteristic of bulk water, and a weight in water of 0.10 g/cm^3 a cell should slide down a vertical interface at a rate of two cell diameters (18 μm) per hour if the contact area is separated from the metal by 100 Å. Since sliding was not observed, the area of contact greatly exceeds 1 μm^2, or the gap is less than 100 Å, or the viscosity of water in the gap exceeds the bulk value, or the surface is not sufficiently smooth to allow sliding. At present we cannot with certainty exclude any of these factors. However, it is likely that the surface of chemically polished polycrystalline lead electrodes is rough at the 1,000 Å level due to the irregular alignment of crystal planes, giving a stepped surface to each crystal (A. Berwick, personal communication). The surface of the mechanically cut lead is presumably a good deal rougher. We hope to pursue this problem and investigate sliding on a truly molecularly smooth metal surface.

We have demonstrated that the adhesion of red blood cells to a metallic surface shows the duplex adhesive behavior characteristic of primary and secondary energy minima which is predicted by the theory of long-range electrostatic and electrodynamic forces. This consistency however does not constitute proof that adhesion is occurring in primary and secondary minima: perhaps only the direct demonstration of a gap would be sufficient. It is possible that components of the cell periphery are reduced at the lead electrode; reduction of sulphydryl for example can occur at the mercury-water interface (Miller et al., 1976). Such reactions might conceivably be responsible for the duplex adhesion seen, both adhesions occurring at "molecular contact." Whatever the mechanism of adhesion, there is no ambiguity in the finding that a large negative surface charge density is necessary to prevent adhesion from occurring. The corresponding repulsive force (Appendix A, Eq. 7) is shown in Fig. 7. The existence of such a long-range repulsion suggests that a similarly long-range attractive force is responsible for pulling the cells onto the metal surface (where short-range attractive forces may subsequently come into play). Calculation of the necessary electrodynamic attractive force is however rendered extremely unreliable because the area of contact is not known. In principle it is possible to circumvent the unknown area if one *assumes* that the change from reversible to irreversible adhesion corresponds to a change from secondary to primary adhesion. If it is further assumed that the repulsive peak of the net

force must be reduced to zero before this change over can take place, the calculated repulsion can be combined with a family of attractive curves, from which the attractive force constant giving the required condition can be selected. This procedure presupposes the algebraic form of the attractive force law. The results however are not particularly enlightening because the corresponding electrostatic repulsion is not sufficiently well characterized, the electrode charge density for the adhesive transition lying somewhere between zero and 5,000 esu/cm^2. Consequently we feel that while our experiment demonstrates long-range electrostatic repulsion, and is strongly suggestive of long-range attraction, a reliable estimate of the size of the attractive force is not yet available.

APPENDIX A

In order to calculate the electrostatic force between the charged electrode and an approaching red blood cell it would seem appropriate to consider the cell's charge density fixed during interaction, while the electrode potential remains constant, since the latter is a conductor. Unfortunately, there is no rigorous treatment for this case. An approximate linearized result (Parsegian and Gingell, unpublished work) was compared with the cases where both interacting surfaces have either constant charge or constant potential, in the linear approximation (Parsegian and Gingell, 1972). Analysis shows that the force for the desired boundary conditions falls between the constant charge and constant potential models but that the three models give widely different force estimates. However, rigorous nonlinear treatments for constant charge (Ohshima, 1974, 1975) and constant potential (Devereux and de Bruyn, 1963) for symmetrical monovalent ions are available. For the conditions of our experiment these methods give virtually identical results from infinity to closer than one Debye length ($\kappa d = 1$) which differ considerably from all linear models. We can consequently utilize either nonlinear method for our purpose.

Eq. 57 of Ohshima (1974) states

$$\xi_h = \frac{2}{(-C + 2)^{1/2}} \left[F\left\{ \frac{2}{(-C + 2)^{1/2}} \middle\backslash \tan^{-1}\left(\frac{|\sigma_1'|}{(-C - 2)^{1/2}} \right) \right\} \right.$$
$$\left. + F\left\{ \frac{2}{(-C + 2)^{1/2}} \middle\backslash \tan^{-1} \frac{|\sigma_2'|}{(-C - 2)^{1/2}} \right\} \right], \quad (7)$$

where $\xi_h \equiv \kappa d$, $\sigma_1' = (4\pi\sigma_1/\kappa\epsilon)(e/kT)$, $\sigma_2' = (4\pi\sigma_2/\kappa\epsilon)(e/kT)$, and $C < -2$. σ_1 and σ_2 are the charge densities on the two surfaces, ϵ is the dielectric constant of water, e is the electronic charge, k is Boltzmann's constant, and T is absolute temperature. F is an incomplete elliptic integral of the first kind defined by

$$F(\alpha/\beta) = \int_0^\beta \frac{d\beta}{(1 - \alpha^2 \sin^2 \beta)^{1/2}}.$$

The interaction force is given by Ohshima (1974) Eq. 54, $P = -nkT(C + 2)$. n = number of ions of either sign per cubic centimeter of solution. This is a standard result (see Verwey and Overbeek, 1948, p. 67). We shall not quote the result of Devereux and de Bruyn (Eq. 2.26) but merely note that that the relation between charge and potential was calculated by the usual method (see Verwey and Overbeek, p. 32, Eq. 12).

$$\psi_m = (2kT/e) \text{ arcsinh } [(q_m/a)/(2\epsilon nkT/\pi)^{1/2}], \tag{8}$$

where q_m is electrode charge from capacitance measurements and a is electrode area.

Brief comment is perhaps necessary before making the identification $\sigma_1 = q_m/a$. Capacitance is defined in terms of a change in charge for a change in potential difference across the capacitor (Eq. 1). Consequently

$$\int_{\Delta\phi(q_m=0)}^{\Delta\phi(q_m)} d\,\Delta\phi = \int_0^{q_m} \frac{1}{C}\, dq_m, \tag{9}$$

$$\Delta\phi(q_m) - \Delta\phi(q_m = 0) = \int_0^{q_m} \frac{1}{C}\, dq_m. \tag{10}$$

Numerical integration of the inverse differential capacitance with respect to electrode charge thus gives not the total PD across the metal-bulk solution interface, but the *difference* in PD across this interface between the state when the electrode bears charge q_m and the state when it bears no charge. It cannot be assumed *a priori* that the PD across the interface at $q_m = 0$ is zero. Dipole contributions due to oriented water may lead to a considerable potential difference (see Bockris and Reddy, 1973, p. 788).

Does this imply that there may be an additional PD across the interface, even at the *pzc*, which will influence an approaching cell—or does the electric field set up by q_m alone completely define the interaction force? In order to answer this question it is necessary to consider the structure of the metal-electrolyte interface in rather more detail. Due to the finite size of hydrated ions, their limit of close approach to the metal defines an outer Helmholtz plane (OHP). The Galvani potential falls from the bulk metal ϕ_m, through this aqueous region, whose dielectric constant is probably only one-tenth that of bulk water, to the OHP where the potential is ϕ_o, then through the Gouy-Chapman diffuse double layer to a value in the bulk of the electrolyte, conveniently designated $\phi = 0$. The total capacitance C_T can be considered to be composed of the capacitance of the inner region between the metal and the OHP, C_I, in parallel with that of the diffuse region C_D (Grahame, 1947).

$$1/C_T = (1/C_I) + (1/C_D). \tag{11}$$

If C_D is calculated using the Gouy-Chapman double layer theory, C_I can be calculated from a knowledge of the measured total capacitance C_T. A curve of C_I as a function of the polarizing voltage can then be constructed from a complete C_T curve. Grahame (1954) made the remarkable discovery that C_I is independent of electrolyte concentration from 0.001 M NaF to 1.0 M NaF for the mercury surface—a fact subsequently verified for lead by Rybalka and Leikis (1966). The value of C_T at any given polarizing potential in any given concentration of NaF can be obtained with great precision from Eq. 11 using the calculated value of C_D and the electrolyte independent value of C_I. This in itself is perhaps the most persuasive evidence for the validity of the Gouy-Chapman treatment of the diffuse double layer. (This is important from our viewpoint, since we will rely on this theory when calculating the electrostatic repulsion using Eq. 7). Thus, at the *pzc* the capacitance of the electrode is composed of an electrolyte independent capacitance due to the inner region and a diffuse region capacitance due to electrolyte, described exactly by Gouy-Chapman theory for the condition $\phi_o = 0$.[2] Therefore we can be sure that when $q_m = 0$, $\phi_o = 0$ and any field due to oriented dipoles, etc., does not itself

---

[2] Gouy-Chapman theory predicts a finite small double layer capacity when the surface charge density is zero.

set up a diffuse double layer; in other words, any dipole field falls to zero potential when the OHP is reached. We can also be confident that this statement holds good for non-zero ϕ_o. Remembering that ϕ represents a difference in potential with respect to the bulk phase, consider the relation

$$\phi_o(q_m) - \phi_o(q_m = 0) = \int_0^{q_m} \frac{1}{C_D} \, dq_m. \tag{12}$$

Since we have just shown that $\phi_o(q_m = 0) = 0$,

$$\phi_o(q_m) = \int_0^{q_m} \frac{1}{C_D} \, dq_m \tag{13}$$

The absolute value of the potential *difference* between the OHP and the bulk electrolyte is, therefore, obtained from the differential capacitance of the diffuse layer. This is the *only* potential which influences an approaching cell: no uncertainty due to dipole potentials enters the problem.

Having established this fact, only one more step is required to show that q_m can be put directly into the repulsion formula (Eq. 7). The charge on the electrode sets up an equal and opposite charge in the mobile double layer, despite the intervening dielectric region, as can be proved by a simple argument involving the continuity of the vector $D \equiv \epsilon(dV/dx)$, where x is the direction perpendicular to the interface. In other words, the double layer which is set up for any given charge density on the metal electrode is the same whether a dielectric region intervenes between metal and electrolyte or not.

Since we have concluded that the potential fall in the double layer set up by the charge q_m is a *complete* description of the potential fall in the diffuse region, the charge on the metal can be imagined to reside at the OHP. This sets up a diffuse double layer whose properties can be reliably calculated, as we have argued, from the Gouy-Chapman theory. Thus q_m divided by electrode area can be equated with surface charge density in Eq. 7.

APPENDIX B

To test our measuring system we made a circuit analogue (Fig. 8) consisting of a high resistance (3.2 MΩ) in parallel with a decade capacitance (1μF maximum) representing the working electrode, and a low resistance (2 kΩ) representing the electrolyte. The circuit analogue passed direct current of the same order as the polarizable electrode. The bridge balance equations give

$$C_1 = \left\{ -\frac{1}{C_B R_B} \pm \left[\frac{1}{C_B^2 R_B^2} - 4w^2 \frac{R_2}{R_1}\left(\frac{R_2}{R_1} + 1\right) \right]^{1/2} \right\} \bigg/ -2w^2 R_2. \tag{14}$$

The negative sign of the root is chosen, such that $C_1 > 0$ always.

In the case in which $R_1 = \infty$ the expression reduces to

$$C_1 = 1/C_B R_B R_2 w^2, \tag{15}$$

which is easily shown to be identical to the normal expression for series capacitance and resistance

$$C_1 = [1/\alpha^2) + 1]C_B, \tag{16}$$

where $\alpha \equiv wC_B R_B$ and $R_B = R_2(1 + \alpha^2)$. The values of components $R_1 R_2 C_1$ were mea-
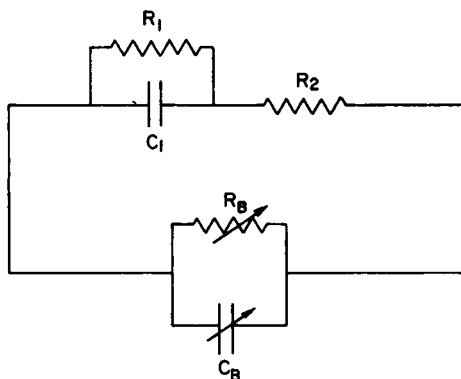
FIGURE 8   Analogue circuit. C_1 is electrode capacitance, R_1 is membrane shunt resistance, R_2 is solution resistance, R_b and C_b are bridge values at balance.

sured separately as functions of frequency from 50 Hz to 10 kHz. R_1 was independent of frequency over this range; R_2 was independent of frequency up to 2 kHz and had increased by only 0.3% by 10 kHz. The value of C_1 alone (nominally 0.8 μF)[3] was practically constant up to 5 kHz and increased by 0.75% by 10 kHz—with a nominal value of 0.1 μF no change in frequency up to 10 kHz was observed.

Using these data for the components of the analogue circuit, the derived value of C_1 was found to remain within +2% of the nominal value of 0.1 μF up to 9 kHz, or within +2% of a nominal value of 0.8 μF up to 5 kHz. In each case apparent dispersion occurred near 9 kHz: its cause was not ascertained, but it was not due to either the DC polarization system or the large DC blocking capacitor. Our measuring system is therefore reasonably well behaved up to 5 kHz when tested on a circuit analogue employing a range of values corresponding to those met experimentally.

We also found that Eq. 16 described our data just as well as the more complete expression (Eq. 14), so the shunt resistance is effectively infinite.

REFERENCES

BANGHAM, A. D., and B. A. PETHICA. 1960. The adhesiveness of cells and the nature of their chemical groups at their surfaces. *Proc. R. Phys. Soc. Edinb.* **28**:43.

BOCKRIS, J. O'M., E. GILEADI, and K. MULLER. 1966. Dielectric relaxation in the electric double layer. *J. Chem. Phys.* **44**:1445.

---

[3]Although the lead electrode can have a capacitance of about 18 μF/cm^2 its area is 0.05 cm^2 so the maximum measured value is $18 \times 0.05 = 0.9$ μF.

BOCKRIS, J. O'M., and A. K. N. REDDY. 1973. Modern Electrochemistry. Vol. 2. Plenum Publishing, London.

CURTIS, A. S. G. 1960. Cell contacts: some physical considerations. *Am. Nat.* **94**:37.

CURTIS, A. S. G. 1962. Cell contact and cell adhesion. *Biol. Rev. (Camb.).* **37**:82.

CURTIS, A. S. G. 1967. The Cell Surface: Its Molecular Role in Morphogenesis. Logos Press Ltd., London.

DERJAGUIN, B. V., I. I. ABRIKOSOVA, and E. M. LIFSHITZ. 1956. Direct measurement of molecular attraction between solids separated by a narrow gap. *Q. Rev. (Lond.)* **10**:295.

DEVEREUX, O. F., and P. L. DE BRUYN. 1963. Interaction of Plane Parallel Double Layers. M.I.T. Press, Cambridge, Mass.

GINGELL, D. 1971. Computed force and energy of membrane interaction. *J. Theor. Biol.* **30**:121.

GINGELL, D., and D. R. GARROD. 1969. Effect of EDTA on electrophoretic mobility of slime mould cells and its relationship to current theories of cell adhesion. *Nature (Lond.).* **221**:192.

GINGELL, D., and V. A. PARSEGIAN. 1972. Computation of the van der Waals interaction in aqueous systems using reflectivity data. *J. Theor. Biol.* **36**:41.

GINGELL, D., and I. TODD. 1975. Adhesion of red blood cells to charged interfaces between immiscible liquids. A new method. *J. Cell Sci.* **18**:227.

GRAHAME, D. C. 1946. Properties of the electrical double layer at a mercury surface. II. The effect of frequency on the capacity and resistance of ideal polarized electrodes. *J. Am. Chem. Soc.* **68**:301.

GRAHAME, D. C. 1947. The electrical double layer and the theory of electrocapillarity. *Chem. Rev.* **41**:441.

GRAHAME, D. C. 1954. Differential capacity of mercury in aqueous sodium fluoride solutions. I. Effect of concentration at 25°. *J. Am. Chem. Soc.* **76**:4819.

GRAHAME, D. C. 1957. Capacity of the electrical double layer between mercury and aqueous sodium fluoride. II. Effect of temperature and concentration. *J. Am. Chem. Soc.* **79**:2093.

GRIFKINS, R. C. 1961. Chemical polishing of lead and its alloys. *Metallurgia.* **63**:209.

GRIGOR'EV, N. B., and D. N. MACHAVARIANI. 1970. Adsorption of thiourea on lead. *Elektrokhimiya.* **6**:89.

Handbook of Chemistry and Physics. 1974. Chemical Rubber Company, Cleveland, Ohio. 54th edition.

KEMP, R. B. 1970. The effect of neuraminidase (3:2:1:18) on the aggregation of cells dissociated from embryonic chick muscle tissue. *J. Cell Sci.* **6**:751.

LE NEVEU, D., R. P. RAND, D. GINGELL, and V. A. PARSEGIAN. 1976. Apparent modification of forces between lecithin bilayers *Science (Wash., D.C.).* **191**:399.

LIFSHITZ, E. M. 1956. The theory of molecular attractive forces between solids. *Sov. Phys. JETP.* **2**:73.

MARUDAS, N. 1975. Adhesion and spreading of cells on charged surfaces. *J. Theor. Biol.* **49**:417.

MILLER, I. R., J. RISHPON, and TENENBAUM. 1976. Electrochemical determination of structure and interactions in spread lipid monolayers. In press.

MINGINS, J., and J. A. G. TAYLOR. 1974. A manual for the measurement of interfacial tension, pressure and potential at air or non-polar oil/water interfaces. Research report of the Technology Group, Unilever Research, Port Sunlight Laboratory, Wirral, Cheshire, England. (This can be obtained from J. Mingins.)

NINHAM, B. W., and V. A. PARSEGIAN. 1970. Van der Waals forces. Special characteristics in lipid-water systems and a general method of calculation based on the Lifshitz theory. *Biophys. J.* **10**:646.

OHSHIMA, H. 1974. Diffuse double layer interaction between two parallel plates with constant surface charge density in an electrolyte solution. II. The interaction between dissimilar plates. *Colloid Polym. Sci.* **252**:257.

OHSHIMA, H. 1975. Diffuse double layer interaction between two parallel plates with constant surface charge density in an electrolyte solution. III. Potential energy of double layer interaction. *Colloid Polym. Sci.* **253**:150.

PARSEGIAN, V. A., and D. GINGELL. 1972. On the electrostatic interaction across a salt solution between two bodies bearing unequal charges. *Biophys. J.* **12**:1192.

PARSEGIAN, V. A., and D. GINGELL. 1973. A physical force model of biological membrane interaction. In Recent Advances in Adhesion. L. H. Lee, editor. Gordon & Breach, New York.

PARSEGIAN, V. A., and B. W. NINHAM. 1969. Application of the Lifshitz theory to the calculation of van der Waals forces across thin lipid films. *Nature (Lond.).* **224**:1197.

PERKINS, R. S., and T. N. ANDERSON. 1969. Potentials of zero charge of electrodes. In Modern Aspects of Electrochemistry. No. 5 J. O'M. Bockris and B. E. Conway, editors. Butterworths & Co. Ltd., London. 203-290.

PINTO DA SILVA, P. 1972. Translational mobility of the membrane intercalated particles of human erythrocyte ghosts. pH dependent aggregation. *J. Cell Biol.* **53**:777.

POWERS, R. W. 1967. An electrochemical cell for microscopic observation of an electrode under polarization. *Electrochem. Tech.* **5**:429.

RYBALKA, K. V., and D. I. LEIKIS. 1966. Study of the structure of the double electric layer on a lead electrode by measuring the differential capacitance. *Electrokhyimiya.* **3**:383.

VASSAR, P. S., J. M. HARDS, D. E. BROOKS, B. HARGENBERGER, and G. V. F. SEAMAN. 1972. Physiochemical effects of aldehydes on the human erythrocyte. *J. Cell Biol.* **53**:809.

VERWEY, E. J. W., and J. T. G. OVERBEEK. 1948. The Interaction of Lyophobic Colloids. Elsevier, Amsterdam.

WEISS, L. 1968a. An experimental and theoretical approach to interaction forces between cells and glass. *Exp. Cell Res.* **53**:603.

WEISS, L. 1968b. Electrophoretic mobility and contact phenomena *Exp. Cell Res.* **51**:609.